Fresenius J Anal Chem (2000) 368 : 4–14

SPECIAL ISSUE PAPER

D. Günther · I. Horn · B. Hattendorf

Recent trends and developments in laser ablation-ICP-mass spectrometry

Received: 6 March 2000 / Revised: 8 May 2000 / Accepted: 11 May 2000

Abstract The increased interest in laser technology (e.g. for micro-machining, for medical applications, light shows, CD-players) is a tremendous driving force for the development of new laser types and optical set-ups. This directly influences their use in analytical chemistry. For direct analysis of the elemental composition of solids, mostly solid state lasers, such as Nd:YAG laser systems operating at 1064 nm (fundamental wavelength), 266 nm (frequency quadrupled) and even 213 nm (frequency quintupled) have been investigated in combination with all available inductively coupled plasma mass spectrometers. The trend towards shorter wavelengths (1064 nm–157 nm) was initiated by access to high quality optical materials which led to the incorporation of UV gas lasers, such as excimer lasers (XeCl 308 nm, KrF 248 nm, ArF 193 nm, and F_2 157 nm) into laser ablation set-ups. The flexibility in laser wavelengths, output energy, repetition rate, and spatial resolution allows qualitative and quantitative local and bulk elemental analysis as well as the determination of isotope ratios. However, the ablation process and the ablation behavior of various solid samples are different and no laser wavelength was found suitable for all types of solid samples. This article highlights some of the successfully applied systems in LA-ICP-MS. The current fields of applications are explained on selected examples using 266 nm and 193 nm laser ablation systems.

Introduction

Laser ablation-ICP-MS has become a powerful and one of the most flexible analytical techniques for direct elemental and isotopic analysis of solids. Over the last 10 years more than 300 publications, addressing the fundamental properties of the ablation process, the transport process of laser-induced aerosols, the ablation cell design and a large number of applications, have been published [see reviews 1–4].

The operating principle of this technique was practically not changed since their introduction by Alan Gray in 1985 [5]. However, the laser wavelength used for ablation, their pulse to pulse stability and the optical arrangement of the beam transfer optics changed significantly.

Laser ablation (LA) is used in two major fields of applications: bulk analysis, with a low spatial resolution, (80–350 μm crater diameter) [6–11] and local analysis with high spatial resolution (4–80 μm diameter) [12–20]. Due to small sample quantities that are removed during laser ablation a high sensitivity is essential for trace and ultra trace analysis. This made the combination of LA and ICP-MS the most attractive and widespread solution. Depending on the application almost all different types of mass filters, such as quadrupole, magnetic sector field (single or double focussing, single or multicollector detectors) and time of flight are used in conjunction with LA and have improved the sequential or simultaneous detection capabilities of LA-ICP-MS, which increased the interest in this direct solid sampling technique [3].

Quantification procedures were significantly improved and accompanied by this, an increasing number of certified solid reference materials, especially for low concentration levels, became available. A variety of calibration techniques have been developed and successfully applied [11, 21–27] to LA-ICP-MS. Additionally, more and more matrix-independent calibration procedures using external reference materials and/or internal standardization procedures have been studied intensively [e.g. 28–30]. Depending upon the calibration strategy used, LA-ICP-MS yields accurate results at a level of < ±5 to ±25% for the determination of concentrations. However, one of the major problems in laser ablation-ICP-MS is the non-sample related variation of the analyte response during the ablation

D. Günther (✉) · I. Horn · B. Hattendorf
Laboratorium für Anorganische Chemie, ETH Zürich,
Universitätsstr. 6, CH-8092 Zürich, Switzerland

process, so-called elemental fractionation. This effect was observed to a certain extent using all types of lasers [31–43]. Individual strategies have been proposed to minimize this effect [27, 35, 44–47]. Until now it is still impossible to separate whether the source of fractionation is related to the ablation process, the transportation process or the excitation and ionization process in the ICP. However, recent observations by Mank and Mason [41] and Russo [43] indicate, that the wavelength of the laser is not the dominant factor with respect to elemental fractionation. Effects of crater diameter to crater depth ratios seem to be more important. This has also been reported using a 193 nm excimer laser ablation system for the purpose of geochronology [27].

Laser ablation systems

Starting in 1985, ruby lasers (694 nm), Nd:YAG lasers (1064 nm, 532 nm, 266 nm, and recently 213 nm) and later excimer lasers (308 nm, 248 nm, 222 nm, 193 nm, and recently 157 nm) were used in LA-ICP-MS. A comparison of the Nd:YAG laser operating at 1064 nm and 266 nm shows better absorption of the UV-wavelength of most samples. The particle sizes produced during ablation are smaller at 266 nm compared to 1064 nm, which is possibly responsible for reduced elemental fractionation observed at 266 nm [32–34]. Experiments comparing the laser beam interaction with solids between 266 nm and 213 nm wavelength [46] show improved ablation characteristics for highly transparent samples. Contrary to other reported work [41, 43], the non-sample related variations of signal intensities with time were found significantly reduced with the shorter wavelength. However, a recently carried out comparison between the wavelengths 266 nm, 213 nm and 157 nm [43] leads to similar elemental fractionation for all three wavelengths. The latter is indicating a smaller influence of the wavelength compared to other parameters, such as energy density, focal point, and crater diameter to depth ratio. A comparison between a 266 nm Nd:YAG laser and a 193 nm excimer laser under closely matched ablation conditions showed better ablation characteristics at 193 nm [10]. These findings may be explained by the differences in particle size distribution produced by the lasers. However, only few investigations have been carried out for wavelengths below 266 nm. Experiments demonstrating the reduced elemental fractionation using a 193 nm ArF excimer laser equipped with a homogenizing optical array have been carried out on ICP-TOFMS. Assuming a separation of elements between particles according to their volatility should result in a significant change in the elemental ratios between fractionating and not fractionating elements within the first seconds of ablation for a stepwise enlarged ablation spot. A schematic of the ablation pattern is shown in Fig. 1. Figure 2 shows obtained elemental ratios (Sr/Zr, Ce/La, Pb/U, Pb/Th, Pb/Pb) in dependence on the crater diameter. Despite the increasing pit sizes (20–120 μm) the ratios obtained are very stable and significant indication for element selective re-deposition on the sample surface is not found. The elemental ratios of Sr/Zr and Ce/La should not change since these elements are considered to be refractory elements and their ablation behavior should therefore be very similar. However, it should be noticed, that the depth to diameter ratio of the ablation crater did never exceed 1. Ablation depths exceeding this aspect ratio show elemental fractionation, which is similar but less pronounced as reported in [27].

Until now, the comparisons between different wavelengths have been carried out on different samples under different output energies, using different optical arrangements, different cell geometries and volumes. The results observed indicate improved ablation behavior for highly transparent samples with lower (deep UV) wavelengths and less matrix-dependent ablation. Some laser parameters and characteristics are summarized in Table 1.

Major differences between the wavelengths used in LA have been observed in their absorption behavior for different solids. The IR wavelength shows excellent absorption for ice and opaque samples, whereas UV laser light shows highly improved absorption on transparent samples such as calcite, fluorite, and quartz [e.g. 20]. The differences in absorption for calcite are illustrated in [46] using a 213 nm Nd:YAG laser. It becomes obvious that the use of 1064 nm, 266 nm or 213 nm Nd:YAG laser or 308 nm (XeCl), 248 nm (KrF) and a 193 nm (ArF) excimer laser

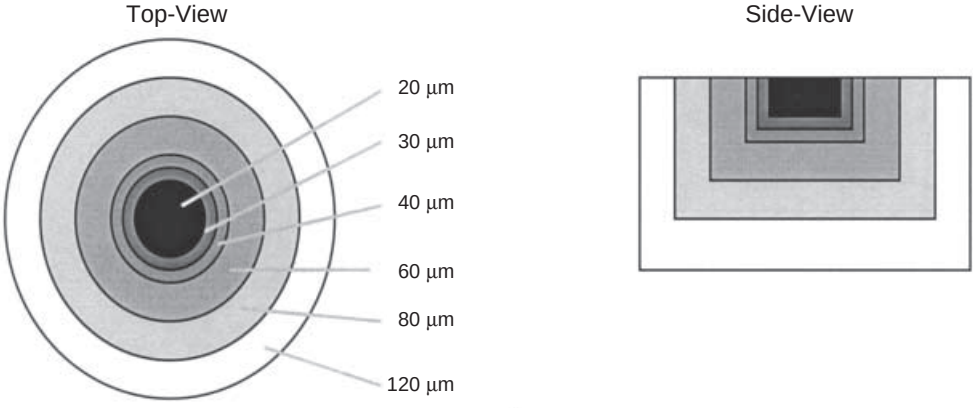

Fig. 1 Schematic cascade ablation using crater sizes of 20 to 120 μm

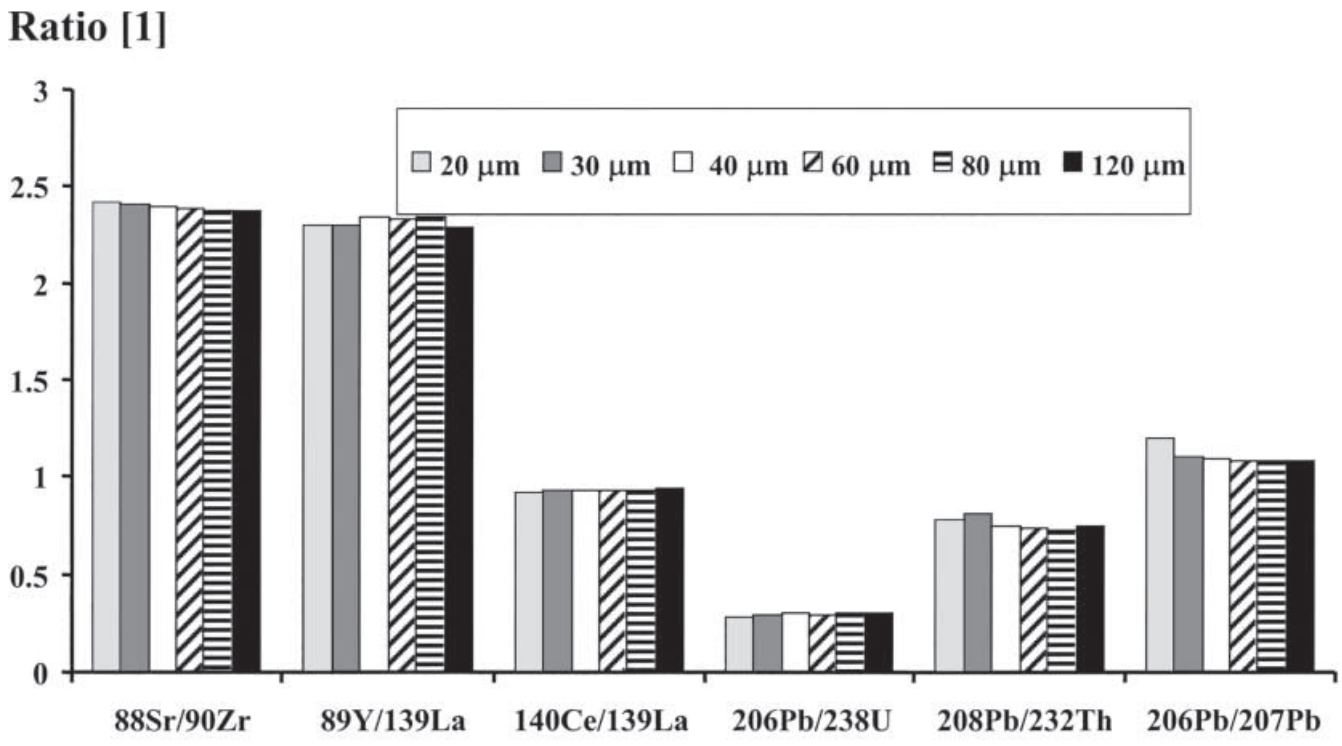

Fig. 2 Elemental ratios measured for various crater sizes on the same ablation spot

depend on the application of interest but there is an obvious trend towards lower wavelengths, as they seem to be more versatile. In geological studies, being still the dominant applications of LA-ICP-MS, 193 nm excimer laser systems have shown to be an advantage [10, 27, 45, 47–54]. New commercially available 193 nm excimer systems directly reflect the growing interest.

New 266 nm Nd:YAG laser based ablation system

It is difficult to study the influence of the laser wavelength on the ablation behavior, the output energy and the optical components implemented into the beam path, separately. Therefore, a 266 nm Nd:YAG laser ablation system, with a similar optical arrangement to that of the existing 193 nm unit was built at the ETH in Zurich. Preliminary experiments were carried out with the aim to study the influence of the wavelength (for equivalent optics) on the ablation characteristic. It is expected that higher energy densities are needed when using 266 nm to obtain results comparable to 193 nm for highly transparent solid materials. In addition to output energy considerations, different wavelength with equivalent optical arrangements should help to clarify the influence of the wavelength on the ablation process. The system consists of a 266 nm Nd:YAG laser (Quantel Brilliant, 1–100 mJ, 266 nm). This laser was first combined to the optical system of the commercially available LSX 200 (Cetac, Omaha, USA). Experiments carried out using 3 mJ on the sample surface and a 100 µm crater show more uniform transient signals than observed at low energy (0.5 mJ). However, the elemental fractionation index calculated [31] was still significant, e.g. 1.5 for the Pb/Ca ratio.

This laser was subsequently combined to an equivalent optical arrangement as described for the 193 nm excimer system [45] and used for preliminary ablation experiments. Figure 3 shows the set-up consisting of a beam expander, homogenizing optics, condenser lens, aperture and refractory objective (10×). The crater structure for 600 laser pulses is shown in Fig. 4. The crater floor is very

Table 1 Typical characteristics of common laser ablation systems

Laser-type	Nd:YAG	Nd:YAG	Nd:YAG	Excimer
Wavelength	1064 nm	266 nm	213 nm	193 nm
Output energy	300–500 mJ	4 mJ	2 mJ	200 mJ
Pulse width	15 ns	9 ns	9 ns	13 ns
Focus position	above surface	below surface	–	image point
Particle size distribution	0.1–10 µm	0.1–3 µm	not reported	0.1–3 µm
Spatial resolution	20–500 µm	5–350 µm	5–200 µm	5–250 µm

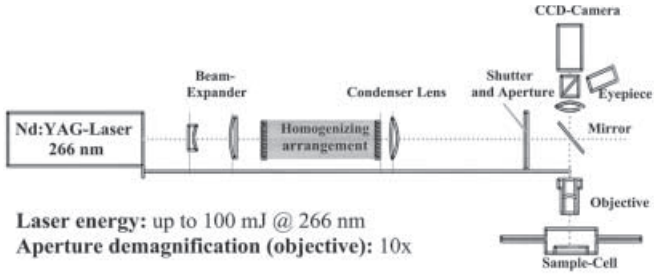

Fig. 3 Schematic view of the homogenized 266 nm Nd:YAG 100 mJ laser system built at ETH Zurich

Fig. 4 SEM photograph of a 100 µm ablation crater in SRM NIST 610 (100 pulses at 70 mJ/pulse laser output)

flat and shows a similar structure to that observed using a 193 nm excimer laser. However, the crater structure is still not as good as for 193 nm. The element ratio of Pb/U observed for 2 different output energies is stable for the ablation sequence shown in Fig. 5. The fractionation index calculated for these ratios is below 1.1 for all elements analyzed here. The fractionation index is calculated by using the background corrected calcium normalized intensities for two adjacent integration intervals of 30 s from a 60 s ablation period and is defined to be the ratio of the second Ca-normalized interval (30–60 s after start ablation) to the first interval (0–30 s). These first experiments indicate that a homogeneous beam profile and fluency are important factors controlling the ablation process and possibly the particle size distribution. However, more detailed experiments have to be carried out to study the ablation process.

Ablation cells

In the middle of the 80s a variety of different ablation cell designs have been developed and tested [56–60] for LA-ICP-OES and LA-ICP-MS. New applications and developments of new ICP source mass analyzers (e.g. time of flight ICP-MS) lead to the construction of various cells, different in volume, geometry and gas flow dynamics. However, the demands on an ideal ablation cell have not changed over the years. A sample of variable size, along with a calibration material, has to be placed into an "airtight" ablation cell. Sample change need to be as easy and fast as possible without disturbance of the ICP conditions. A strategy for ablation cell geometry optimization is given in [60]. The volume of the ablation cell and the transportation tube is influencing the dispersion and the sample density in the ICP. Smaller cell volumes

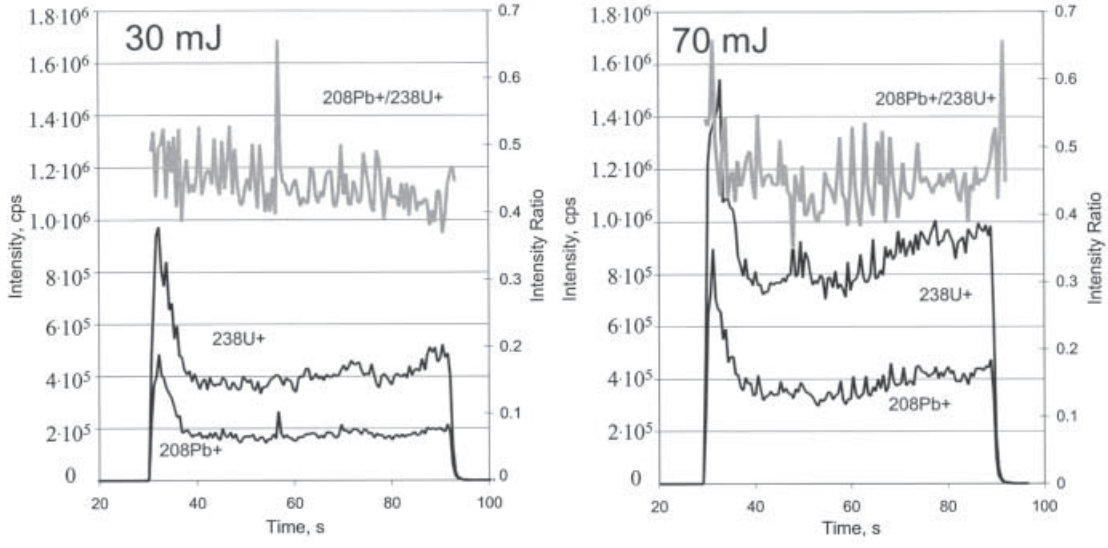

Fig. 5 Ablation signals for Pb and U with a homogenized high power 266 nm Nd:YAG laser

(below 1 cm^3) reduce "sample-washout" time of the cell. A high carrier gas speed through the cell and transfer tubes reduces material deposition in the system, reducing memory effects and increasing transport efficiency. Transportation phenomena are almost negligible if ablation is performed directly into the ICP as shown for LA-ICP-OES [61]. This set-up can mainly be applied to bulk analysis because sample observation using microscope optics is difficult.

A more recently investigated ablation cell (jet-cell) directs the ablation gas flow of argon through a capillary onto the side of ablation [27, 62], which improves signal stability. In general, the wide variety of samples requests various ablation cells optimized to the application of interest and almost every laboratory using this technique is working with two or more ablation cells.

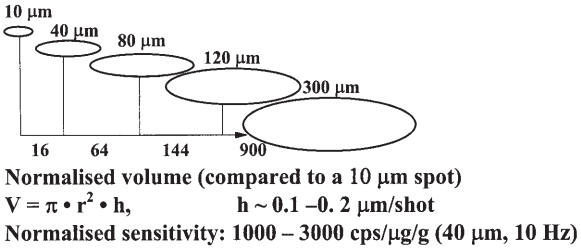

Fig. 6 Volume and mass dependence on different crater diameters, which are responsible for sensitivity in LA-ICP-MS

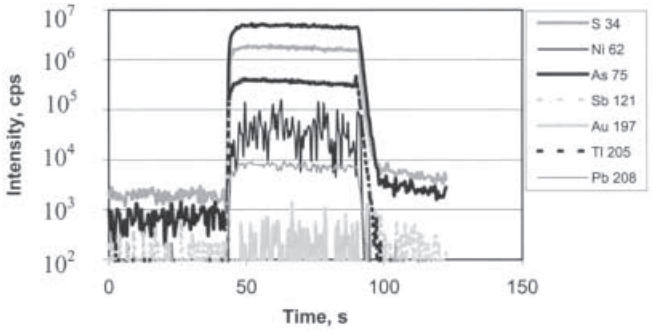

Fig. 7 Transient signal of a multielement analysis on minerals. Example shown for marcasite (FeS_2)

ICP-MS for laser ablation

Since laser ablation offers the possibility for bulk and local analysis, the demands on the flexibility of ICP-mass spectrometers are tremendous. In bulk analysis the spatial resolution is between 0.1 to 1 mm whereas local analyses require a resolution between < 5 and 50 μm. That gives a difference in the volume of 900, assuming a constant ablation rate per pulse for a 10 μm crater compared to a 300 μm crater (Fig. 6). Therefore, the linear dynamic range of the detector is one of the most important parameter for solid sampling. Major elements, usually used as internal standards for quantification, ideally are to be measured together with minor and trace elements. Few commercially available systems are equipped with pulse counting and analogue mode amplifiers in the detection system resulting in 9–10 orders of magnitude in linear dynamic range. Figure 7 shows a typical linear dynamic range needed for a 40 μm spot mineral analysis.

Analyte sensitivity, as reported for different instruments, is mainly influenced by the crater size, energy density and repetition rate used in these experiments, which influences the amount of ablated and transported material. Normalizing sensitivities that were obtained with similar energy density to a crater diameter of 40 μm and a repetition rate of 10 Hz lead to rather equal sensitivities of ~1000–3000 cps ng^{-1} g for most commercial instruments. The limits of detection are therefore mainly influenced by the background noise. Typical limits of detection for a standard instrument in combination with LA are given in Fig. 8.

Another critical parameter for multielement analysis is the data acquisition speed, extensively discussed in [63]. Recent improvements in sector-field instruments (which have commonly been viewed as slow with respect to magnet jump speed) have been implemented. Measurement efficiency was improved by a short and fast change of the accelerator voltage for a magnet-jump, so that the differences between the quadrupole based instruments and sector field instruments are within a factor of 2 [64]. The ideal detection for short transient signals in laser ablation

Fig. 8 Typical limits of detection for major (**a**) and trace elements (**b**) for a crater diameter of 40 μm (10 Hz, 1.2 mJ) measured on a NIST 610 using an ELAN 6100 DRC in standard mode

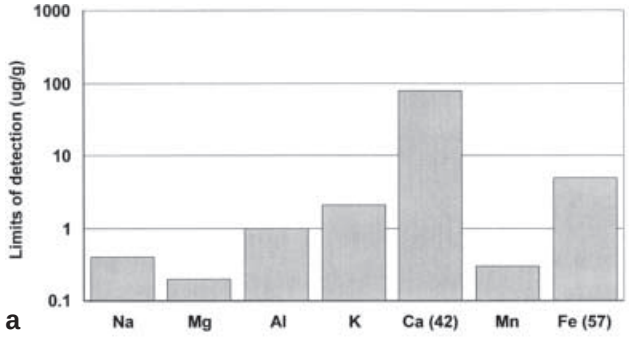

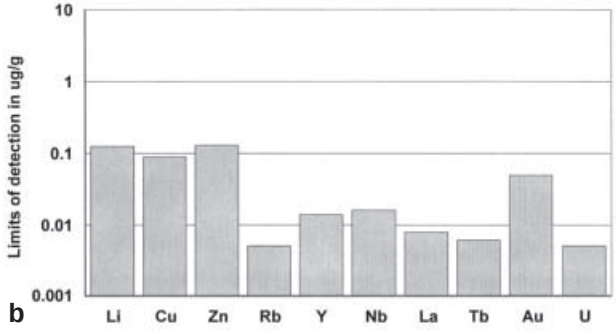

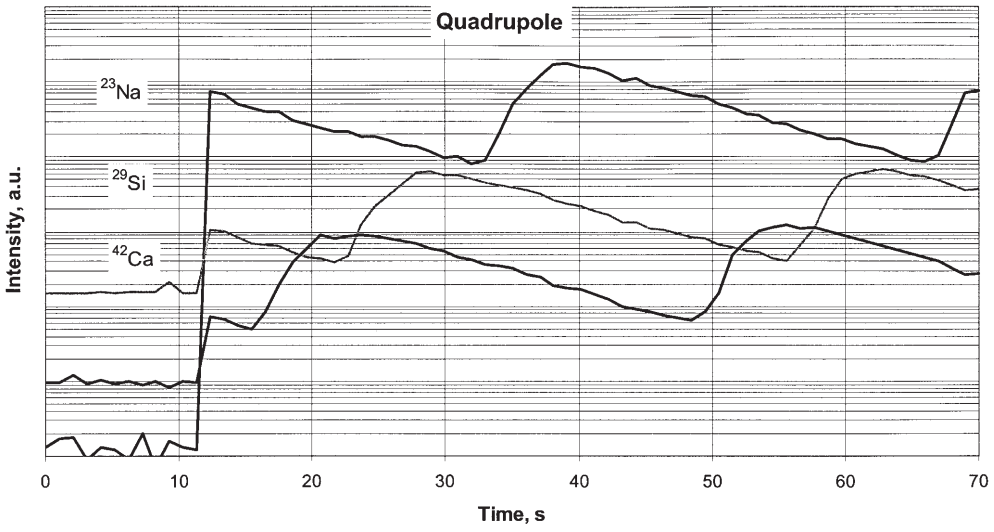

Fig. 9 Drastically enhanced spectral skew, as observed for a scanning instrument, when the laser induced signal variation is modulated by the scanning frequency. A combination of a laser frequency of 1 Hz and scan duration of 1.03 s leads to transient signals as shown. The delays between two maxima in the transient signals are inversely proportional to the difference between pulse delay and scan duration (33 s)

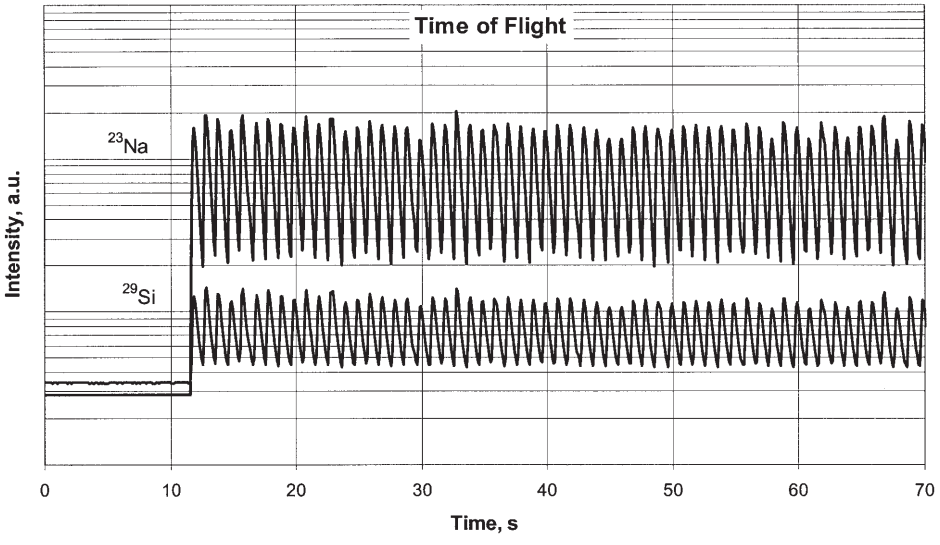

Fig. 10 Single shot ablation using LA in combination with ICP-TOFMS (102 ms dwell time per isotope). Selection of 2 isotopes shown out of a 60 isotope menu (1 Hz ablation)

would be an "all-collecting" sector-field instrument where a detector array is placed in the space and time focus that collects all isotopes fully simultaneously. ICP-TOFMS though is becoming very close to the ideal, because all isotopes are sampled at the same time and detection is very fast [65, 66]. The typical sampling time of such an instrument is in the range of 5 μs, and with a readout time of 12.75 ms (255 spectra averaged) the problem of spectral skew (Fig. 9), occurring for sequential mass analysis, is eliminated (Fig. 10). This provides access to elemental composition even for ultra-short transient signals and precise isotope ratios.

This high data acquisition speed is necessary for fast transient concentration variable signals, occurring for example during the ablation of fluid inclusions. Here, spectral skew might lead to analyte loss from heterogeneously distributed tiny crystals. Another application is depth profiling, where the fast and simultaneous data acquisition allows accurate determination of the drill time through different coatings or layers [66]. However, the sensitivity and spectral background need some improvements to increase the capabilities of such instruments for high spatial resolution analysis in the very low ng/g concentration region.

Mixed gas sample introduction

The ablation process has been studied under different gas environments to increase the sample transport into the ICP-MS. Different gas combinations, e.g. nitrogen, hydrogen and helium [10, 12, 40, 42, 67], have been investigated. The use of nitrogen is leading to higher sensitivity in the high mass region, which is especially of importance for the determination of Pb and U. Eggins and co-worker [40] reported increased sensitivity (high mass region) by adding ~300 mL helium to the main flow of argon flushing the ablation cell. The improvement of sensitivity is

mainly related to decreased material deposition around the ablation crater. However, using pure helium as an ablation cell carrier gas which is subsequently mixed with argon showed increased sensitivity and reduced background intensities and therefore improved limits of detection [10]. The degree of improvements is different for 266 nm and 193 nm laser ablation systems. However, the source of this enhancement (which might be related to the particle size distribution or a change in ICP conditions) is still not quantified and needs further investigation. All mixed gas experiments (especially using helium) change the gas dynamics in the interface, which makes it very difficult to rule out specific processes being responsible for the effects described for alternative carrier gases for sample introduction.

Selected applications of LA-ICP-MS using a 193 nm excimer ablation system

Mineral analyses. Laser ablation-ICP-MS has been used for a variety of trace element studies in different types of minerals. Matrix-independent calibration possibilities have led to many new insights into geological processes. Table 2 shows a comparison between electron microprobe analysis and laser ablation-ICP-MS data, which were acquired on identical samples. The accuracy between the two independent analytical methods is further evidence for the applicability of non-matrix match calibration as a quantification procedure for LA-ICP-MS.

Bulk analysis. The analysis of trace elements in rock powder samples fused with lithium tetraborate with matrix-matched standards has been studied in detail [6, 9]. The

Table 2 Comparison between electron microprobe analysis and LA-ICP-MS analysis performed on a variety of minerals

Mineral and sample	Element	EMP wt-%	LA-ICP-MS wt-%	Int. Std.
Amphibole (UM33/GE35P)	Na_2O	1.7	1.35– 1.5	SiO_2
	Al_2O_3	16	16	SiO_2
	CaO	13	12–13.5	SiO_2
	TiO_2	1	1.0	SiO_2
Clinopyroxene (GR17.3)	Al_2O_3	7	6.8	SiO_2
	CaO	25.5	24–25.9	SiO_2
(159.2)	Al_2O_3	3.6	3.8	SiO_2
	CaO	25.3	25.2	SiO_2
Andradite (GR17.3)	Al_2O_3	4.3–6	5.1	SiO_2
	CaO	33	31	SiO_2
Apatite (GR2)	SiO_2	0.12–0.24	0.12–0.26	CaO
Zirconolite (159.2)	Al_2O_3	0.45	0.6–0.7	CaO
	TiO_2	35	38	CaO
	ZrO_2	33–36	~20–60	CaO
	Ce	0.78–1.14	0.58–0.86	CaO
	Nd	1.0 –1.34	1.02–1.18	CaO
	Sm	0.24–0.6	0.46–0.59	CaO
	Y	2.35–6.13	3.86–5.44	CaO
Zircon (UM33/GE35P)	ZrO_2	65–67	40–63	SiO_2
	Y_2O_3	0.10–0.15	0.10	SiO_2

Table 3 Results obtained on different lithium tetraborate fused reference materials using non matrix matched calibration and Li as internal standard

	Andesite AGV-1			Basalt JB-2			Rhyolite RGM-1		
	Ref. value µg/g	this work µg/g	SD	Ref. value µg/g	this work µg/g	SD	Ref. value µg/g	this work µg/g	SD
Li		447893	3717		I.S.			I.S.	
Mn	713	762	11	1680	1709	11	309	282	5
Y	19.6	19.9	0.2	21.3	24.9	0.4	25	24.54	0.51
Zr	229	243	1.8	44.5	51.5	0.7	219	241	4
La	36.3	42.3	0.5	2.11	2.56	0.10	24	25.55	0.89
Lu	0.23	0.28	0.01	0.35	0.51	0.05	0.41	0.45	0.03
Hf	5.32	5.55	0.5	1.64	1.77	0.31	6.2	6.32	0.4
Th	5.5	6.6	0.4	0.24	0.35	0.05	15.1	15.75	0.51
U	1.84	1.9		0.15	n.d.		5.8	5.59	0.3

See Ref. [68], SD: standard deviation, I.S.: internal standard, n.d.: not detectable

use of an internal standard element (determined prior to the laser analysis by XRF) leads to good agreement between certified and determined values. Further experiments have shown that the determination of Li as matrix element using a lithium tetraborate fused reference material (e.g. AGV-1), and subsequently applying this value as internal standard for other fused rock samples have been successful. Table 3 contains a selected number of elements using non-matrix matched calibration and Li as internal standard. This quantification procedure will allow using LA-ICP-MS as a routine technique for trace element determination in lithiumtetraborate fused powder samples. The homogeneity of such samples has been investigated and is considered to be better than 15% RSD for sub μg/g and better than 5% for concentrations above 1 μg/g. However, as shown in [9] the matrix blank needs to be analyzed for each individual sample run.

The application of LA-ICP-MS for the determination of elemental ratios [69], which is important for a wide variety of new materials (e.g. Zeolites), was successfully tested. Zeolites of different Si/Al stoichiometry were analyzed by LA-ICP-MS and subsequently digested for determination by solution nebulisation ICP-OES. A selection of LA-ICP-MS and solution ICP-OES data is summarized in Table 4. The element ratios were calibrated using SRM NIST 610.

The determination of elemental and isotopic ratios is also widely used for the purpose of geochronology, whereby the U/Pb decay series are used to determine the crystallization or metamorphic age of a mineral. Mainly accessory phases such as zircon and monazite have been dated by an in-situ analytical technique with sufficient precision and accuracy. So far SHRIMP (sensitive high-resolution ion microprobe) has been used exclusively for high spatial resolution age determinations of minerals [70]. Nowadays it is also possible to achieve similar precision and accuracy of better than 2% RSD (95% confidence interval) by LA-ICP-MS as it has been described by several authors [12, 27].

Direct solution ablation. Laser ablation-ICP-MS is too expensive to be the method of choice for solution analysis. However, introduction of synthetic solutions and dual sample introduction systems for laser-induced aerosols mixed with liquids (dried and wet) were used to overcome the lack of solid reference materials for quantification [21–27]. A specific sample preparation procedure was proposed by [71] to modify the absorption of aqueous solutions, used as calibration standards in LA of solids. However, the ablation behavior of solutions is wavelength dependent, in contrast to IR light, which is transmitted to a high degree in diluted solutions and therefore requires additives or modifiers to perform direct ablation analysis [23]. UV light such as 193 nm is absorbed by the same solutions without modifications. In a study, high matrix containing solutions (0.1 g/L Sn) were ablated. Samples were filled into polyethylene micro-tubes, sealed and placed in the ablation cell to minimize evaporation and cross-contamination. The laser was imaged onto the tube, and an 80 μm hole (2 mJ pulse energy, 10 Hz repetition rate) was ablated. The transient signal obtained by the direct ablated liquid is shown in Fig. 11.

The major difference between the solid and liquid ablation is the stability of the signal, which is worse for liquids due to droplet splashing during the ablation. Quantification was carried out using identically prepared synthetic solutions for calibration (500 μg/g multielement standards, Merck, Germany). The accuracy of the determination of 1 μg/g and the related limits of detection are summarized in Tables 5 and 6. A total amount of 11 μL of

Table 4 Comparison of Si/Al-ratios between ICP-OES and LA-ICP-MS on 2 different zeolithes using SRM NIST 610/Zeolithe for calibration

	LA-ICP-MS				ICP-OES	
Repeat Zeolithe #1	Si/Al-ratio Calibration NIST610	RSD	Si/Al-ratio Calibration Zeolithe	RSD	Si/Al-ratio	RSD
1	21.7		22.1			
2	21.8		22.6			
3	21.8		22.2			
4	22.2		22.3			
5	22.2		22.6			
Average	22.0	1.10%	22.4	1.05%	22.0	1.60%
Repeat Zeolithe #2	Si/Al-ratio Calibration NIST610	RSD	Si/Al-ratio Calibration Zeolithe	RSD	Si/Al-ratio	RSD
1	5.62		5.88			
2	5.63		6.08			
3	5.64		5.66			
4	5.92		6.04			
5	5.67		5.94			
Average	5.7	2.20%	5.92	2.80%	5.81	1.40%

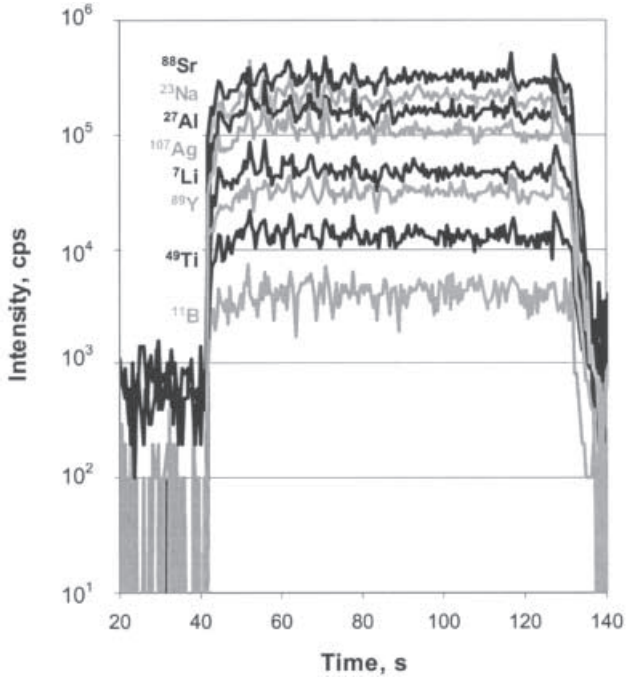

Fig. 11 Signals for ablation of a 0.5 µg/g multielement solution (matrix: 1 mg/g Sn) out of a polyethylene tubing. Splashing of droplets from the opening crater leads to rather noisy signals

solution was determined 3 times from the same tube, which leads to absolute limits of detection of 2 pg. The major advantage of such an ablation procedure is the very low sample uptake, the greatly reduced spectral interferences and matrix effects. Elemental fractionation in solution ablation was not observed. The limits of detection are in the ng/g range for most of the elements. However, very small sample volumes can be analyzed and easily calibrated. In addition, this ablation strategy might be useful for the investigation of spectral interferences in laser ablation.

Local analysis. Local analyses of all types of inclusions are of major interest in laser ablation and a lot of studies have been carried out to get access to their elemental composition [13–20, 54]. Laser ablation in combination with ICP-TOFMS offers new capabilities to study the isotopic and elemental composition of inclusions (see Fig. 12). The heterogeneous composition of such micro inclusions (vapor, liquid, and solid crystals [16] might lead to loss of crystals during the opening procedure with the laser and/or detection using a quadrupole based ICP-MS. This may not be important when measurements are carried out for 25 or less isotopes but becomes a major concern if the time per sweep gets too long. However, most inclusions have an unknown elemental composition and they might contain more elements as detected so far. In these cases there is no second chance since the inclusion is consumed in a single analysis. Therefore, the "quasi" simultaneous detection of 60 and more isotopes using an ICP-TOFMS will help to get more representative elemental ratios

Table 6 Limits of detection for direct liquid ablation of a 1 mg/g Sn matrix (10 Hz, 80 µm spot)

Limits of detection (ng/g)			
Li	0.7	Cu	1.0
B	3.0	Ga	0.2
Na	11	Sr	0.7
Mg	1.8	In	0.5
Al	3.9	Ba	1.8
K	19	La	0.1
Ti	16	Nd	0.3
V	3.4	Sm	0.7
Mn	2.0	Hf	0.4
Co	0.1	Tl	0.4
Ni	1.2	Pb	1.3
Zn	1.7	U	0.7

Table 5 Determined concentrations of a 1 µg/g solution in a 1 mg/g Sn solution using direct liquid ablation

Element	Concentration µg/g	RSD	Element	Concentration µg/g	RSD
Li	1.02	6%	Cu	1.01	5%
B	1.03	4%	Ga	1.06	3%
Na	1.25	1.8%	Sr	1.04	1%
Mg	1.0	2%	In	0.99	5%
Al	1.05	1%	Ba	0.93	3%
K	0.92	8%	La	1.04	1%
Ti	0.89	10%	Nd	1.06	1%
V	0.88	2%	Sm	1.03	2%
Mn	0.98	3%	Hf	1.03	1%
Co	1.01	1%	Tl	0.95	1%
Ni	0.91	2%	Pb	0.95	2%
Zn	1.03	1%	U	1.01	1%

RSD: relative standard deviation

which will lead to better reproducibility of the results after quantification.

Quasi non-destructive analysis. The analyses of plants, gold [72, 73] and gemstones [74] to "fingerprint" the origin of these materials have been studied in detail and showed the great potential of LA-ICP-MS. However, the degree of destruction prevented this technique from real applications considering the damage to an already polished gemstone. Studies carried out in our laboratory show that the homogeneous energy distribution on the sample surface using a 120 µm crater allows to remove 60 nm layers with very controlled conditions using few laser pulses. This damage, visible only under an electron microscope still allows the successful fingerprinting of gemstones. The constant ablation of 20 pulses leads to 1.2 µm damage to the sample, which can easily be polished off after analysis or may be placed at a location where it is of no concern. Figure 13 shows SEM picture of 1, 2 and 3 pulses onto an aluminium oxide matrix. More than 15 elements could be detected.

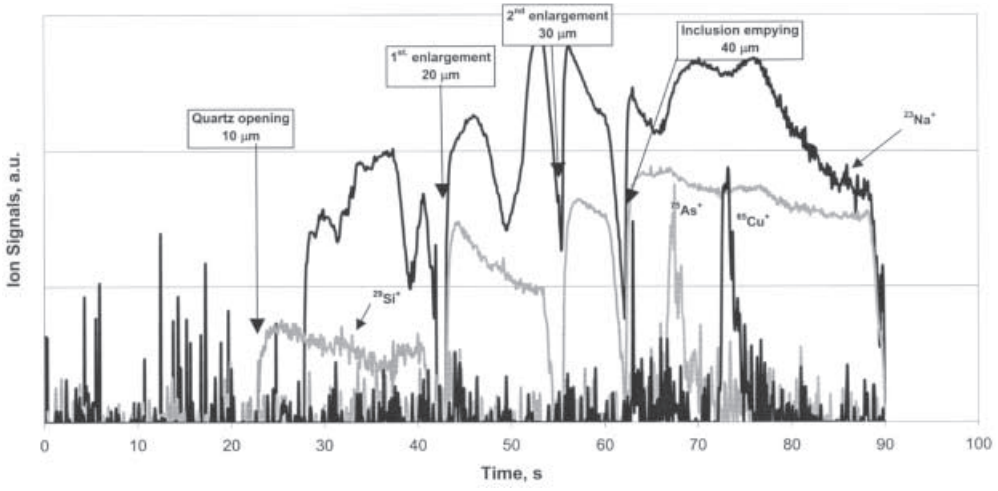

Fig. 12 Transient signal of a 35 µm fluid inclusion opened with increasing pit sizes

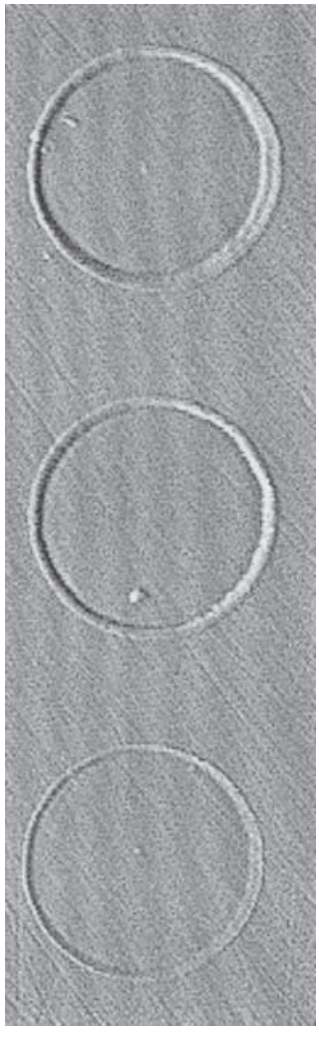

Fig. 13 SEM picture after 1, 2 and 3 pulses per crater onto aluminium oxide (60 nm removal per shot) to determine degree of destruction of a gemstone sample

Summary and outlook

Laser ablation-ICP-MS is possibly the fastest growing analytical technique for major, minor, trace element analysis of solids and isotope ratio determinations. Many of the drawbacks have been investigated in detail and tremendous improvements were achieved. This has directly led to steadily increasing interest and broader acceptance of this micro-analytical technique. Starting as a powerful tool for trace element determinations in geological applications the method has matured to an applicable routine technique for material science, biology, archaeology, medicine, and forensic.

It is expected that instrumentation will be simpler in the set-up and in operation. A higher degree of automation with respect to sample changers and data reduction will eventually lead to industrial application, such as process and quality control. The influence of wavelength, transport efficiency and fractionation will continue to be major research topics in the future.

Acknowledgements This paper is dedicated to the 60th birthday of H.P. Longerich. SEM pictures prepared by Eric Reusser (Institute of Mineralogy and Petrography) and support for the equipment by ETH Zurich are acknowledged.

References

1. Moenke-Blankenburg L (1993) Spectrochim Acta Rev 15: 1
2. Darke SA, Tyson JF (1993) J Anal At Spectrom 8: 145
3. Durrant S (1999) J Anal At Spectrom 14: 1385
4. Günther D, Jackson SE, Longerich HP (1999) Spectrochim Acta Rev 54: 381
5. Gray A (1985) Analyst 110: 551
6. Odegard M, Hamester M (1997) Geostand Newslet 21: 245
7. Bédard LP, Baker DR, Machado N (1997) Chem Geol 138: 1
8. Odegard M (1999) Geostand Newslet 23: 173
9. Becker JS, Dietze HJ (1999) Fresenius J Anal Chem 365: 429
10. Günther D, Heinrich CA (1999) J Anal At Spectrom 14: 1369
11. Reid JE, Horn I, Longerich HP, Forsythe L, Jenner GA (1999) Geostand Newslet 23: 149
12. Hirata T, Nesbitt RW (1995) Geochim Cosmochim Acta 59: 2491
13. Shepherd TJ, Chenery SR (1995) Geochim Cosmochim Acta 59: 3997
14. Moissette A, Shepherd TJ, Chenery SR (1996) J Anal At Spectrom 11: 177
15. Audetat A, Günther D, Heinrich CA (1998) Science 279: 2091
16. Günther D, Audétat A, Frischknecht R, Heinrich CA (1998) J Anal At Spectrom 13: 263

17. Ghazi AM, McCandIess TE, Vanko DA, Ruiz J (1996) J Anal At Spectrom 11: 667
18. Ulrich T, Günther D, Heinrich CA (1999) Nature 399: 676
19. Schäfer B, Günther D, Frischknecht R, Dingwell DB (1999) Eur J Mineral 11: 415
20. Audetat A, Günther D (1999) Contrib Min Pet 137: 1
21. Chenery SR, Cook JM (1993) J Anal At Spectrom 8:299
22. Cromwell EF, Arrowsmith P (1995) Anal Chem 67: 131
23. Günther D, Frischknecht R, Müschenborn HJ, Heinrich CA (1997) Fresenius J Anal Chem 359: 390
24. Günther D, Cousin H, Magyar B, Leopold I (1997) J Anal At Spectrom 12: 165
25. Falk HF, Hattendorf B, Krengel-Rothensee K, Wieberneit N, Dannen SL (1998) Fresenius J Anal Chem 362: 468
26. Leach JJ, Allen LA, Aeschlimann DB, Houk RS (1999) Anal Chem 71: 440
27. Horn I, Rudnick RL, McDonough FM (2000) Chem Geol 164: 281
28. Jackson SE, Longerich HP, Dunning GR, Fryer BJ (1992) Can Min 30: 1049
29. Chen Z, Doherty W, Grégoire DC (1997) J Anal At Spectrom 12: 653
30. Horn I, Hinton RW, Jackson SE, Longerich HP (1997) Geostand Newslet 21: 191
31. Fryer BJ, Jackson SE, Longerich HP (1995) Can Min J 33: 303
32. Jeffries TE, Perkins WT, Pearce NJG (1995) Analyst 120: 1365
33. Motelica-Heino M, Donard OFX, Mermet JM (1999) J Anal At Spectrom 14: 675
34. Motelica-Heino M, Le Costumer P, Thomassin JH, Gauthier A, Donard OFX (1998) Talanta 46: 407
35. Chen Z (1999) J Anal At Spectrom 14: 1823
36. Outridge PM, Doherty W, Gregoire DC (1997) Spectrochim Acta 52B: 2093
37. Doherty W, Outridge PM, Grégoire DC (1996) J Anal At Spectrom 11: 1123
38. Figg D, Kahr MS (1997) Appl Spectrosc 51: 1185
39. Figg DJ, Cross JB, Brink CH (1998) Appl Surf Sci 287: 127–129
40. Eggins SM, Kinsley LPJ, Shelley JMG (1998) Appl Surf Sci 129: 278
41. Mank AJG, Mason PRD (1999) J Anal At Spectrom 14: 1143
42. Jeong SH, Borisov OV, Yoo JH, Mao XL, Russo AE (1999) Anal Chem 71: 5123
43. Russo R, Borisov O, Mao X, Liu H (2000) W1 2000 Wint Conf Plasma Spectrochem, Ft Lauderdale, p 164
44. Hirata T (1997) J Anal At Spectrom 12: 1337
45. Günther D, Frischknecht R, Heinrich CA, Kahlert H-J (1997) J Anal At Spectrom 12: 939
46. Jeffries TE, Jackson SE, Longerich HP (1998) J Anal At Spectrom 13: 935
47. Günther D, Heinrich CA (1999) J Anal At Spectrom 14: 1363
48. Von Quadt A, Günther D, Frischknecht R, Zimmermann R, Franz G (1997) Schweiz Mineral Petrog Mitt 77: 265
49. Sylvester PJ, Eggins SM (1997) Geostand Newslet 21: 215
50. Sylvester PJ, Ghaderi M (1997) Chem Geol 141: 49
51. Eggins SM, Rudnick RL, McDonough WF (1998) EPSL 154: 53
52. Sinclair DJ, Kinsley LPJ, McCulloch MT (1998) Geochim Cosmochim Acta 62: 1889
53. Glaser SM, Foley SF, Günther D (1999) Lithos 48: 263
54. Garofalo P, Audetat A, Günther D, Heinrich CA, Ridley J (2000) American Min 85: 78
55. Stalder R, Ulmer P, Thompson AB, Günther D (2000) American Min 85: 68
56. Carr JW, Horlick G (1982) Spectrochim Acta 37B: 1
57. Arrowsmith P, Hughes SK (1988) Appl Spectroscopy 42: 1231
58. Ishizuka T, Uwanmino Y (1983) Spectrochim Acta 38B: 519
59. Schrön W (1986) Patent DD 153 921 B1
60. Moenke L, Gäckle M, Günther D, Kammel J (1990) R Soc Chem, Cambridge, Special Pub 85: 1
61. Liu XR, Horlick G (1994) Spectrochim Acta 50B: 537
62. Jackson SE, Sterling R (1999) personal communication
63. Longerich HP, Jackson SE, Günther D (1996) J Anal At Spectrom 11: 899
64. Pesch R, Hamester M, Wills J (2000) FP32 2000 Wint Conf Plasma Spectrochem, Ft. Lauderdale, p 274
65. Mahoney PP, Li GQ, Hieftje GM (1996) J Anal At Spectrom 11: 401
66. Bleiner D, Plotnikov A, Vogt C, Wetzig K, Günther D (2000) Fresenius J Anal Chem (submitted)
67. Durrant S (1992) Analyst 117: 1585
68. Govindaraju K (1994) Geostand Newsl 18: 158
69. Rings S, Sievers R, Jansen M (1999) Fresenius J Anal Chem 363: 165
70. Compston W (1999) Mineral Mag 63:297
71. Buoe-Bigne F, Masters BJ, Crighton JS, Sharp BL (1999) J Anal At Spectrom 14: 1665
72. Watling RJ, Lynch BF, Herring D (1997) J Anal At Spectrom 12: 195
73. Watling RJ (1998) J Anal At Spectrom 13: 917
74. Guillong M (2000) Diploma Thesis, ETH Zurich